

The formation of planetary systems: from the ISM to planets

Ana I. Gómez de Castro
Instituto de Astronomía y Geodesia (CSIC-UCM)
Universidad Complutense de Madrid,
Madrid, E-28040, Spain

Alain Lecavelier
Institute d'Astrophysique de Paris

Miguel d'Avillez
University of Evora

Jeffrey L. Linsky
JILA, University of Colorado, Boulder, CO 80309-0440 USA

José Cernicharo
DAMIR-IEM-CSIC

September 24, 2008

Abstract

Planetary systems are angular momentum reservoirs generated during *star formation*. Three of the most important problems in contemporary astrophysics require the understanding of this process:

The physics of the ISM. Stars form from dense molecular clouds that contain a $\sim 30\%$ of the total interstellar medium (ISM) mass. The structure, properties and lifetimes of molecular clouds are determined by the overall dynamics and evolution of a very complex system — the ISM. Understanding the physics of the ISM is of prime importance not only for Galactic but also for extragalactic and cosmological studies. Most of the ISM volume ($\sim 65\%$) is filled with diffuse gas at temperatures between 3000 K and 300,000 K, representing about a 50% of the ISM mass.

The physics of accretion and outflow. Powerful outflows are known to be involved in the regulation of the angular momentum transport during star formation: the so-called accretion-outflow engine. Elementary physical considerations point out that, to be efficient, the acceleration region for the outflows must be located close to the star (within 1 AU), where the gravitational field is strong. According to recent numerical simulations, this is also the region where terrestrial planets could form after 1 Myr. We should keep in mind that today

the only evidence for life in the Universe comes from a planet located in this inner disk region (at 1 AU) from its parent star. The temperature of the accretion-outflow engine is between 3000 K and 10^7 K. After 1 Myr, during the classical T Tauri stage, extinction is small and the engine becomes naked and can be observed at ultraviolet wavelengths.

The physics of planet formation. Observations of volatiles released by dust, planetesimals and comets provide an extremely powerful tool for determining the relative abundances of the vaporizing species and studying the photochemical and physical processes acting in the inner parts of the protoplanetary disks. This region is submitted to the strong UV radiation field produced by the star and the accretion-ejection engine. Absorption spectroscopy provides the most sensitive tool to determine the properties of the circumstellar gas as well as the characteristics of the atmospheres of the inner planets transiting the stellar disk. UV radiation also pumps the electronic transitions of the most abundant molecules (H_2 , CO,...) that are observed in the UV.

In summary, access to the UV range is instrumental to make progress in this field since the resonance lines of the most abundant species in the Universe in the temperature range from 3000 K to 300,000 K are observed in the ultraviolet, as well as the electronic transitions of the most abundant molecules (H_2 , CO, OH, CS, S_2 , CO_2^+ , C_2 , O_2 , O_3 ...). In addition, a UV mission provides the most efficient mean to measure the abundance of Ozone in the atmosphere of the thousands of transiting planets expected to be detected by the next space missions (GAIA, Corot, Kepler...). Thus a follow-up UV mission would be optimal to identify Earth-like candidates.

UV astronomy, ISM, pre-main sequence stars, jets, winds, accretion disks, planets

1 Introduction

The formation of planetary systems covers a broad range of physical (and astrophysical) processes ranging from the physics of star formation at large (the interstellar medium (ISM), molecular clouds, initial mass function), to the physics of accretion and outflow (accretion disk properties, winds generation, disk instabilities) and finally, the formation of planets (dust nucleation, planetesimal and planet formation, planetary differentiation, planetary atmospheres and sustainable biological systems). The objective of this article is to summarize the reasons why access to the UV range is instrumental to make progress in this area of astrophysics.

For this reason, the article has been splitted into three key sections: physics of the ISM, physics of accretion and outflow, and planets and biomarkers. A summary has been added to the end of this contribution with the required UV capabilities to make progress in the field.

Table 1: Components of the ISM (reference properties)

Component	n (cm^{-3})	T (K)	Ionization fraction	Spectral range
HIM	few 10^{-3}	$(5 - 10) \times 10^6$	1	X-ray, UV
WIM ^(a)	few 10^{-1}	$10^{4(b)}$	1	UV, Radio, Optical
WNM	1-10	$(3 - 8) \times 10^3$	0.1	UV, Optical, IR, Radio
CNM	1-50	20-100	10^{-2}	UV, IR, Radio
MM	$10^3 - 10^6$	10	$< 10^{-4}$	IR, Radio

- (^a) In the last few years, a new subclassification has been introduced to distinguish between the WIM envelope around molecular clouds so-called McKee & Ostriker WIM or MOWIM and the rest, so-called, Reynolds WIM.
- (^b) This nominal temperature is often assigned because most of the observations come from H α emission however, UV observations have pointed out the presence of significantly hotter gas traced by C IV or OVI.

2 The physics of the ISM

Understanding the physics of the ISM is of prime importance not only for Galactic but also for extragalactic and cosmological studies. The ISM is everything observable in the Galaxy except for stars, *e.g.*, gas (in many different phases: ionized, atomic, molecular), dust, high energy particles (*e.g.* cosmic rays), and magnetic fields. Henceforth, the ISM is a very complex, highly non-linear dynamical system whose evolution controls star formation and metallic mixing and, therefore, the chemical enrichment of the Universe.

The ISM is often classified into five components: Hot Ionized Medium (HIM), Warm Ionized Medium (WIM), Warm Neutral Medium (WNM), Cold Neutral Medium (CNM) and dense molecular medium (MM) (see *e.g.* Kulkarni & Heiles, 1988); the diffuse components (HIM, WIM, WHM and CNM) seem to be in pressure equilibrium. The main properties of these components are summarized in Table 1. X-ray observations are the most sensitive to the very hot gas with temperatures $T \geq 10^6$ K. IR and radio wavelengths represent the only mean to study the dense molecular gas where stars do form. UV spectroscopy is the most sensitive tool to determine the properties (column densities, temperatures, ionization fractions, metallicity, depletion etc..) of the diffuse gas in the 3000-300,000 K temperature range, *e.g.*, WNM and WIM.

In the last few years, old models, based on pressure equilibrium between the various ISM phases (*e.g.* McKee & Ostriker, 1977) have been replaced by detailed numerical simulations that allow studying the ISM as it is: a dynamical system. High spatial resolution numerical simulations now permit addressing a set of problems simultaneously, encompassing both large and small scales, provided that the appropriate grid size, resolution and numerical tools (*e.g.*

adaptive mesh refinement) are used. To name just the most important problems, global modelling yields information on the formation and lifetimes of molecular clouds, how star-forming regions are influenced by large-scale flows in the ISM, and which dynamic roles that SNe and superbubbles play in triggering local and global star formation (see Heyer & Zweibel, 2004).

Key problems in ISM physics include the determination of the relative contribution to the energy input from the various possible sources (SNe, massive star winds and radiation fields, mass infall from the halo, galactic dynamics, cosmic rays and magnetic fields) and the role of MHD turbulence and shocks in the energy cascade and structure formation. During the last years, a very efficient feed-back loop has been set between radio observations and numerical simulations to study the role of MHD turbulence in the energy cascade within the densest regions of the ISM (HI and molecular clouds). A similar feed-back loop needs to be set with UV observations to understand the heating/cooling processes and the overall ISM evolution, including the formation of molecular clouds.

Numerical simulations predict that $\sim 65\%$ of the ISM volume (within the disk: $|z| < 250$ pc) is filled with gas at temperatures between 10^3 K and $10^{5.5}$ K; in particular WIM ($10^4 < T < 10^{5.5}$ K) is expected to fill 25% of the disk volume while HIM filling factor is smaller (17 %) because it escapes to the halo (de Avillez & Breitschwerdt, 2004). These predictions agree with recent observations. The Wisconsin H-Alpha Mapper (WHAM) has observed O III emission extending to galactic latitudes as high as $|b| \sim 45^\circ$ and even He I ($\lambda 5876\text{\AA}$) emission has been detected. On the contrary, X-ray and extreme UV observations are pointing out that the filling factor of the HIM in the local ISM is small. Clearly, UV facilities are required to make progress in our understanding of the physics of the galactic ISM. This physics can be studied at two scales:

Large scale (> kpc scale):

At this scale, the prime objectives are understanding the overall star formation efficiency and which parameters control the disk-halo circulation (the Galactic fountain). The roles of supernova explosions, expanding H II regions and the overall galactic dynamics (shear, spiral arm shocks, high velocity cloud shocks...) is examined in detail. Some attention is also devoted to understand galactic magnetic fields and the galactic dynamo.

Small scale (the Local Bubble scale):

The Local Bubble represents the nearest region of the ISM and thus, an ideal laboratory to test the *details* of the ISM physics: dust depletion and abundances, non-equilibrium ionization, shocks, turbulence, etc.

2.1 Halo-disk interaction in the Milky Way

The Milky Way is surrounded by a large halo of hot gas which must be replenished as the gas cools. The most direct evidence comes from the detection of high ionization UV resonance lines (e.g., OVI 1031 \AA and CIV 1549 \AA) and of

X-ray emitting gas surrounding the Galactic disk. The X-ray halo has a luminosity of $\sim 4 \times 10^{39}$ erg s^{-1} , and the thickness of the emission is probably a few kpc. The temperature of the X-ray emitting gas is $1 - 2 \times 10^6$ K, well below the escape temperature and thus gravitationally bound to the Galaxy. The high temperatures of the gas in the halo can only be explained by energetic processes, most likely occurring in the Galactic disk, although external sources could also contribute. The most likely energy sources for these processes are massive OB stars.

There is also evidence that hot halo gas has cooled, as provided by the presence of the high-ionization UV resonance lines. Some of the UV resonance lines might be produced by photoionization of gas near 10^4 K, but there is good evidence that the high ionization lines, such as SiIV 1396, 1402Å, CIV 1548, 1550Å, and NV 1238, 1242Å are due to gas that is now cooling (Savage & Sembach 1994). The ratio of column densities obtained from the SiIV and CIV absorption lines is almost constant, implying that the ionization state of the gas is nearly identical in different parts of the halo. Benjamin & Shapiro (1993) argued that in a Galactic fountain, gas cooling from 10^6 K would be opaque to its own radiation, causing it to self-ionize, so that its ionization state is determined by the cooling process itself. They also showed that the absorption strength of NV is reproduced by this model. Martin & Bowyer (1990) have shown that the emission from CIV and OIII ions is consistent with being produced from a cooling Galactic fountain.

The fountain is a dynamic process, which involves a flow time scale, that can be much shorter than any of the microphysical time scales due to ionization and recombination. The gas escaping into the halo has an initial temperature well in excess of 10^6 K, where the assumption of collisional ionization equilibrium (CIE) is approximately valid. This means that the rate of ionizations per unit volume through collisions between ions and electrons equals the rate of recombinations per unit volume. As the hot plasma expands away from the disk it will cool adiabatically thereby reducing its temperature and density (to be of the order of 10^{-2} cm^{-3}). Thus, the probability of three body collisions is very small. However, in the case of proper balancing, collisional ionization ought to be compensated by three body recombination, one electron recombining and the other taking up the released energy in form of kinetic energy. Instead, radiative recombination is much more probable. Since both collisional ionization and radiative recombination are cooling processes for the plasma, departures from CIE are inevitable. Breitschwerdt & Schmutzler (1999) have shown that in this case recombination of highly ionised species lags behind and occurs mainly at considerable heights from the disk.

Figure 1 shows the distribution of various ionization stages in non-equilibrium ionization (NEI) for an ion like oxygen can be. Care should be taken in using a single ion like O^{5+} as a diagnostic element for plasma temperature should, because its ionization fraction can be almost constant over two orders of magnitude in temperature, while in CIE O^{5+} traces gas with $T > 10^5$ K, having a peak at 3×10^5 K (see also Schmutzler & Tscharnuter 1993).

Thus, measurements of the z-dependence of OVI, NV, CIV and SiIV emission

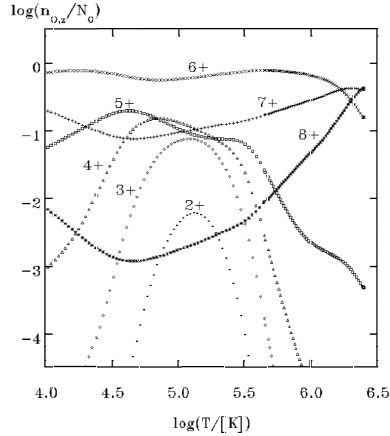


Figure 1: Ionization stages of Oxygen in a self-consistent calculation of a galactic outflow (wind) (Breitschwerdt & Schmutzler 1999). The initial temperature of the flow is $T = 2.5 \times 10^6$ K.

are of prime importance for determining whether the the gas is in collisional equilibrium ionization, in non-equilibrium ionization, or whether other relevant heating sources maybe present. These observations are critically needed to constrain numerical models of the ISM in disk galaxies providing further clues on how matter and energy are transferred within the Galaxy. This is clearly displayed in Figure 2; adaptative mesh simulations of the dynamical evolution of the ISM (Avillez & Breitschwerdt 2004, 2005) show that matter in the disk is concentrated in dense shells and filaments while the halo acts as a pressure release valve for the hot ($T > 10^{5.5}$ K) phase in the disk thus controlling its volume filling factor. The upper parts of the thick ionized disk form the disk-halo interface located around 2 kpc above and below the midplane, where a large scale fountain is set up by hot ionized gas, injected there either from gas streaming out of the thick disk or directly from superbubbles in the disk underneath, escaping in a turbulent convective flow.

Radio observations can be used to map the clumpy distribution of matter in the disk, but the most important constraints will come from the study of the vertical distribution of warm gas, which is studied with UV spectroscopy. This is also true for the high velocity clouds (HVCs) detected by their HI 21 cm, which are surrounded by hot ionized envelopes as pointed out by the new observations from the Far Ultraviolet Spectroscopic Explorer (FUSE) mission and the Space Telescope Imaging Spectrograph onboard the Hubble Space Telescope (HST/STIS). The detection of O VI, C IV and Si IV absorption indicates that many HVCs have a hot, collisionally-ionized component (Danly et al 1992, Tripp et al 2003). UV absorption lines provide detailed information on the physical conditions and abundance in the gas. Understanding the ionization of such envelopes will permit us to constrain the properties of the Galactic corona and

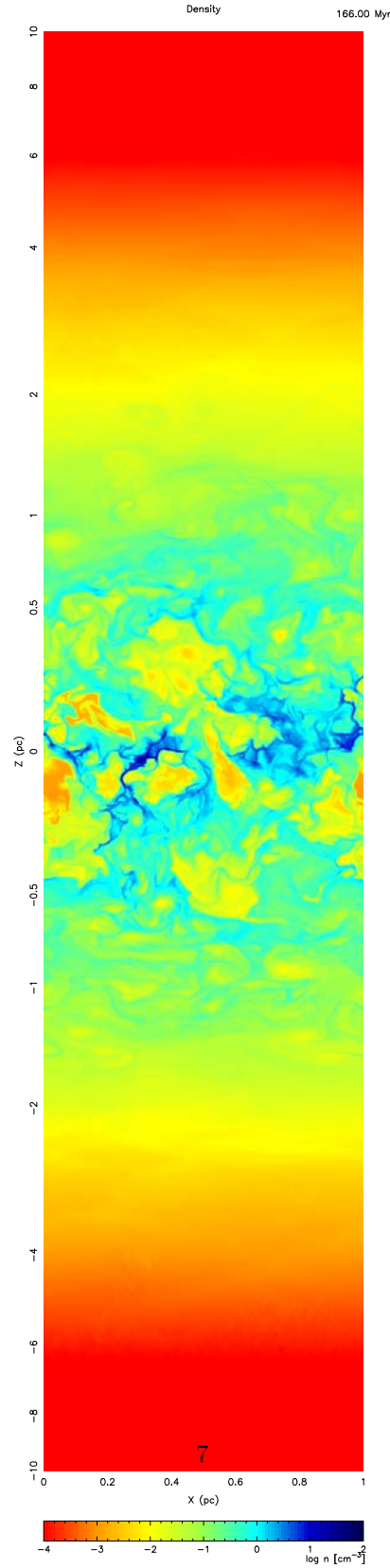


Figure 2: Slice through the 3D data set showing the vertical (perpendicular to the midplane) distribution of the density at time 166 Myr. Red/blue in the colour scale refers to lowest/highest density (or highest/lowest temperature). The z -scale above 0.5 and below -0.5 kpc is shrunk (in order to fit the paper size) and thus, the distribution of the labels is not uniform (from Avillez & Breitschwerdt 2005).

the Local Group medium. UV absorption lines are the most sensitive probes for determining the abundances (and henceforth the Galactic or extragalactic origin) of the HVCs (see e.g. Richter et al 2001). Note that the most robust species for constraining the metallicity of HVCs is O I since oxygen is only slightly depleted by dust grains (Moos et al 2002) and the ionization potential of OI is very similar to the H I. Thus oxygen abundances based on the OI/HI ratio depend only on the ionization of the gas for substantially ionized plasmas.

2.2 The local ISM

The Sun lies inside the Local Bubble, a large ionized gas bubble that extends outwards from the Sun to a neutral hydrogen column density $\log N(HI) \approx 19.2$ corresponding to a geometrical size of 100–200 pc, depending on the direction from the Sun. The Local Bubble’s morphology has been identified by Na I absorption, which is formed in the cold gas that surrounds the Local Bubble and determines its shape (Lallement et al. 2003). The Local Bubble is thought to be an H II region formed by the explosions of supernovae and the strong winds of young hot stars in the Lower Centaurus Crux subgroup of the Scorpio-Centaurus Association (Maíz-Apellániz 2001; Berghöfer & Breitschwerdt 2002). The temperature of the gas in the Local Bubble is estimated to be about 10^6 K if most of the soft X-ray background is due to thermal emission from the Local Bubble gas, but analysis of extreme ultraviolet emission obtained with the CHIPS satellite has not yet led to an accurate temperature or emission measure for the hot, low density Local Bubble gas, which may be far out of ionization equilibrium.

Embedded in the Local Bubble are a number of warm gas clouds. The Sun is located inside one of these clouds called the Local Interstellar Cloud (LIC). The LIC was first identified by Lallement & Bertin (1992) on the basis of measured Doppler shifts of interstellar absorption lines in many directions that are consistent with a single velocity vector, implying that all of the gas in this cloud is moving with a common velocity away from the center of the Sco-Cen Association. Analysis of UV interstellar absorption lines with the high resolution echelle gratings in the GHRS and STIS instruments on HST enabled Redfield & Linsky (2000) to determine a temperature of the LIC gas (7000 ± 1000 K) and morphology of the LIC. The LIC center is located in the anti-Galactic center direction. The maximum column density of the LIC is $\log N(H I) = 18.3$, the LIC’s maximum dimension is about 6.8 pc, and its mass is about $0.32 M_{\odot}$. The main evidence for the Sun being located inside the LIC is that the neutral helium flowing into the heliosphere, which is not influenced by the solar wind, has the same temperature and flow vector as the LIC (Witte 2004).

Slavin & Frisch (2002) computed the ionization of many elements in the LIC taking into account UV and EUV radiation from the most important ionizing source, the star ϵ CMa, hot white dwarfs and other contributing stars, the diffuse UV background, and the estimated radiation from the putative conductive boundary between the warm clouds and the hot gas of the Local Bubble. More sensitive UV observations are required to study this boundary layer. Their

models assumed ionization equilibrium and realistic hydrogen column densities between the center of the LIC and the external sources of ionizing radiation. One of their models predicts the temperature, electron density, and ionization of many elements in good agreement with observations. Dust, which is present in the LIC and other nearby warm clouds, plays an important role in cooling the gas and in depleting metals such as iron from the gas phase.

There are a number of other warm, partially ionized clouds in the solar neighborhood which are also located inside the Local Bubble. The so-called G cloud identified by Lallement and Bertin (1992), which is situated in the Galactic Center direction, is slightly cooler than the LIC, and has a somewhat different velocity vector. The closest star α Cen (1.3 pc) is located in the G cloud but shows no evidence for absorption by gas at the LIC velocity even in very high signal-to-noise GHRS echelle spectra. This places an upper limit of 0.05 pc for the thickness of the LIC in the direction of α Cen and a time of $< 3,000$ years for the Sun to leave the LIC and enter either the G cloud or an unknown interface region between the LIC and the G cloud.

The broad UV spectral coverage, high spectral resolution, and accurate wavelength scale of the STIS instrument allowed Redfield & Linsky (2004) to measure absorption line wavelengths, widths, and Doppler shifts for many atoms and ions including H I, D I, C II, N I, O I, Mg II, Al II, Si II, and Fe II along 29 different lines of sight through warm clouds in the Local Bubble. They detected absorption at 50 different velocities along these lines of sight, indicating about 12 clouds with different velocity vectors. The observation of absorption lines from elements or ions with very different atomic weights (2 for deuterium compared to 56 for iron) allowed Redfield and Linsky (2004) to solve for the gas temperature and nonthermal motions (turbulence) separately. They found velocity components in the local ISM with temperatures as high as about 12,000 K and a few components with temperatures below 3000 K. The mean temperature is 6680 ± 1490 K, which is characteristic of warm clouds, but there are some velocity components inside the Local Bubble that could be cold clouds. In almost all cases the nonthermal motions are far smaller than the thermal motions. The mean thermal pressure in the clouds, $P_T/k = 2280 \pm 520$ K cm⁻³. The magnetic fields in these clouds have not yet been measured.

While STIS spectra of interstellar absorption lines formed in the local ISM have begun to reveal its secrets, we have sampled far too few lines of sight to identify the structure of the local ISM in any detail. In particular, we do not yet have a good understanding of the amount of gas at different temperatures in the local ISM, nor do we have a detailed understanding of how the ionization and temperature of the gas depends on the radiation environment and past history. Understanding the physics of the local ISM is required if we are to have any confidence in understanding the physics of the Galactic disk, halo, and ISM in other galaxies. Since most interstellar absorption lines are located in the UV and the absorption lines are typically narrow with multiple velocity components, a future sensitive high resolution UV spectroscopic mission is needed to extend the preliminary work provided by the GHRS and STIS instruments on HST.

3 The physics of accretion and outflow

Understanding how stars form out of the contracting cores of molecular gas is a major challenge of contemporary astrophysics. Angular momentum must be conserved during gravitational contraction and magnetic flux is built up and dissipated in the process, the underlying mechanisms are still under debate.

Solar-like protostars are an excellent laboratory for this purpose since their pre-main sequence (PMS) phases last ~ 100 Myr. The collapse of low-mass protostars is subalfvénic, thus these protostars are expected to be magnetized. The detection of kG fields in stars as young as a few million years (Guenter et al 1999, Johns-Krull et al 1999) supports this assumption. In the last few years, a new paradigm has emerged to understand the basics of star formation. Protostars are assumed to be magnetized and star growth is regulated by the interaction between the stellar magnetic field and the disk. The physics of this interaction is outlined in Figure 3. The disk-star interaction basically transforms the angular momentum of the disk (differential rotation) into plasmoid which are ejected from the system. There is a current sheet that separates two distinct regions: an inner stellar outflow and an external disk flow. Magnetic flux dissipation should occur in the current layer producing the ejection of plasmoid, as well as the generation of high energy particles (cosmic rays) in the environment leading to generation of X-rays and ultraviolet radiation.

The phenomenon is non-stationary and controlled by two different temporal scales: the rotation period and the magnetic field diffusion time scale. Stellar rotation is a well known parameter that controls the opening of the field lines towards high latitudes. Plasmoid ejection however, is controlled by field diffusion which is poorly determined (see e.g. Priest & Forbes 2000). All models can be fitted into this basic configuration (Uzdensky 2004).

In the last 5 years, numerical research on this interaction has gone into an outburst (see e.g. Goodson et al 1997,1999). So far most of the studies have analyzed the interaction between a dipolar stellar magnetic field and a Keplerian accretion disk. Numerical simulations show that the fundamental mechanism for jet formation is robust. The star-disk-outflow system is self-regulating when various initial disk densities, stellar dipolar field strengths and primordial fields associated with the disk are tested (Matt et al 2002), although strong stellar magnetic fields may disrupt the inner parts of the accretion disk temporarily (Kueker et al 2003). Despite the numerical advancements so far, the real properties of the engine itself are poorly known because of the lack of observations to constrain the modelling. Very important questions still open include:

1. How does the accretion flow proceed from the disk to the star? Is there any preferred accretion geometry as, for instance, funnel flows?
2. What role do disk instabilities play in the whole accretion/outflow process?
3. What are the dominant processes involved in wind acceleration? What

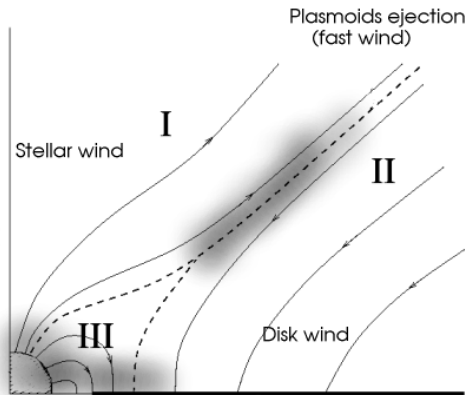


Figure 3: The interaction between the stellar magnetic field and the disk twist the stellar field lines due to the differential rotation. The toroidal magnetic field generated out of the poloidal flux and the associated pressure tends to push the field lines outwards, inflating them and eventually braking the magnetic link between the star and the disk (boundary between regions I and II). Three basic regions can be defined: Region I dominated by the stellar wind, Region II dominated by the disk wind and Region III dominated by stellar magnetospheric phenomena. The dashed line traces the boundaries between this three regions. The continuous lines indicate the topology of the field and the shadowed areas represent regions where magnetic reconnection events are likely to occur producing high energy radiation and particles (from Gómez de Castro 2004).

are the relevant time-scales for mass ejection?

4. How does this high energy environment affect the chemical properties of the disk and planetary building?
5. Whether and how this mechanism works when radiation pressure becomes significant as for Herbig Ae/Be stars?

Infrared and radio wavelengths cannot access this engine, because the spatial scales involved are tiny (< 0.1 AU or 0.7 mas for the nearest star forming regions; for instance ALMA resolution is 10 mas) and the temperatures are too high (3000 – $300,000$ K). High resolution IR spectroscopy has indeed confirmed the presence of *warm* molecular gas with temperatures of 1500 – 3000 K in the innermost disk: both CO (fundamental and overtone) and H₂O emission have been detected (see Najita et al 2000 for a review or Carr, Tokunaga & Najita 2004 for more recent results). Fortunately, after 1 Myr, *e.g.* from the classical T Tauri Star (CTTS) phase, the circumstellar extinction is small ($A_V <$

1 mag) and the engine described above can be properly tested at ultraviolet wavelengths. The UV spectral range is the richest for diagnosing astrophysical plasmas in the 3000-300,000 K temperature range: the resonance lines of the most abundant species are located in the UV. In addition, as the UV radiation field is strong in the circumstellar environment, fluorescence emission from the most abundant molecules (H_2 , CO, OH, CS, S_2 , CO_2^+ , C_2 , CS) is observed. As a result, a single high resolution spectrum in the 1200–1800 Å range provides information on the molecular content, on the abundance of very reactive species such as the O I, and on the warm and hot gas associated with the CTTS. The potentials of the UV to study the physics accretion during the pre-main sequence evolution are outlined below.

3.1 UV observations of the jet engine in low mass stars

The engine is a small structure (≤ 0.1 AU) with several different constituents (the accretion flow, the stellar magnetosphere, the winds and the inner part of the accretion disk) all radiating in the ultraviolet. The UV spectrum of the T Tauri Stars (TTSs) has a weak continuum and many strong emission lines. The continuum is significantly stronger than that observed in main sequence stars of similar spectral types (G to M); the so-called optical-veiling represents the low energy tail of this excess UV emission (Hartigan et al 1990). The underlying photosphere is barely detected, and only in warm (G-type) weak line TTSs (WTTSs) is the photospheric absorption spectrum observed. The UV continuum excess is significantly larger in the CTTSs than in the WTTSs, as is well illustrated in the colour (UV-V) – magnitude (V) diagram displayed in Figure 4. Simple models of hydrogen free-free and free-bound emission added either to black bodies or to the spectra of standard stars reproduce reasonably well the UV continuum (Calvet et al 1984; Bertout et al 1988; Simon et al 1990). The fits yield electron temperatures of 1×10^4 - 5×10^4 K which are chromospheric-like. Three different mechanisms have been proposed to generate this hot plasma: (1) the UV continuum could originate in dense chromospheres (Calvet et al 1984), (2) in the release of the gravitational binding energy from the infalling material (Bertout et al 1988; Simon et al 1990; Gullbring et al 2000), or (3) in the outflow (Ferro-Fontán & Gómez de Castro, 2003; Gómez de Castro & Ferro-Fontán, 2005). This uncertainty points out why high resolution UV spectroscopy (and monitorings) are so crucial to understand and constraint the physics of the engine.

3.1.1 Signatures of accretion

The most obvious signature of accretion is the detection of narrow red-shifted absorption components on top of the emission profiles of singly ionized species such as Mg II or Fe II. It is widely accepted that this absorption is produced in funnel flows: magnetic tubes connecting the inner disk to the stellar surface. However there are no detailed maps of the funnel flows except for some attempts made in the optical range (Petrov et al 2001; Bouvier et al 2003). UV mapping

excess is not produced by the accretion shock. Whether the wind or an extended magnetosphere is responsible for the UV continuum excess is still a matter of debate. In fact the “coexistence” of several funnel flows has been proposed to explain this fact (Muzerolle et al. 2001).

3.1.2 Signatures of disks

High resolution HST/STIS spectra have revealed, for the first time, the rich UV molecular emission in CTTS. H₂ fluorescence emission has now been studied in detail in the nearest CTTS, TW Hya, and the richness of the spectrum is overwhelming: Herczeg et al (2002) detected 146 Lyman-band H₂ lines, representing 19 progressions (see Figure 4)! The observed emission is likely produced in the inner accretion disk, as are the infrared CO, H₂O lines. The excitation of H₂ can be determined from the relative line strengths by measuring self-absorption in lines originating in low-energy lower levels, or by reconstructing the Ly α emission line profile incident upon the warm H₂ using the total flux from each fluorescing upper level and the opacity in the pumping transition. Using this diagnostic technique, Herczeg et al (2004) estimated that the warm disk surface has a column density of $N_{H_2} = 3.2 \times 10^{18} \text{ cm}^{-2}$, a temperature of $T=2500 \text{ K}$, and a filling factor of H₂ as seen from the source of the Ly α emission of 0.25 ± 0.08 . The observed spectrum shows that some ground electronic state H₂ levels with excitation energies as large as 3.8 eV are pumped by Ly α . These highly excited levels may be formed by dissociative recombination of H₃⁺, which in turn may be formed by reactions involving X-rays and UV photons from the star. A quick inspection of the UV spectra in the IUE and HST Archives shows that fluorescent H₂ UV lines are observed in most of the TTSs (see also Gómez de Castro & Franqueira 1997b; Valenti et al. 2000; Ardila et al. 2002).

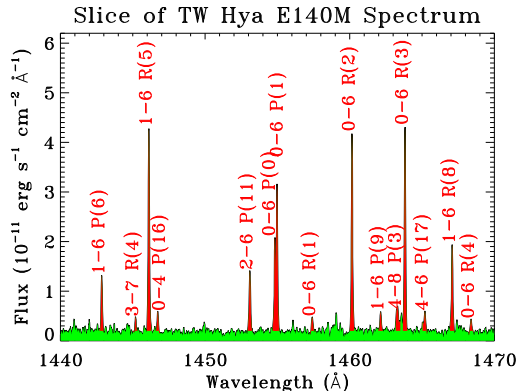


Figure 5: A portion of the HST/STIS spectrum of the CTTS TW Hya. The narrow H₂ emission lines originate in the B electronic state after being pumped by the HI Ly α line (from Herczeg et al 2002).

The role of far-UV radiation fields and high energy particles in the disk chemical equilibrium is now beginning to be recognized. Bergin et al 2003 have shown how strong Ly α emission may contribute to the observed enhancement of CN/HCN in the disk. The penetration of UV photons coming from the engine in the dusty disk could produce an important change in the chemical composition of the gas allowing the growth of large organic molecules. In this context, UV photons photodissociating actual organic molecules at $\lambda > 150$ nm could play a key role in the chemistry of the inner regions of the disk while those photodissociating H₂ and CO will control the chemistry of the external layers of the disk directly exposed to the radiation from the central engine (see, e.g. Cernicharo 2004).

Strong continuum FUV emission (1300-1700 Å) has been detected recently in some stars with bright molecular disks including GM Aur, DM Tau, and LkCa 15, together with inner disk gaps of few AUs (Bergin et al. 2004). This emission is likely due to energetic photoelectrons mixed into the molecular layer pointing to the presence of a very hot component in the disk. This very hot component is probably created by X-ray and high energy particle irradiation of the disk (Glassgold et al 2004; Gómez de Castro & Antonicci, 2005).

Spectroscopic observations of volatiles released by dust, planetesimals and comets provide an extremely powerful tool for determining the relative abundances of the vaporizing species and studying the photochemical and physical processes acting in the inner parts of the protoplanetary disks. Ultraviolet observations of comets show the enormous possibilities of UV spectroscopy for this purpose (see Brosch et al. 2005). Ultraviolet radiation also plays a very important role in the evolution of the primary atmospheres of the planetary embryos.

3.1.3 Signatures of winds

Large scale outflows are observed as collimated jets or Herbig-Haro objects in some TTSs (see Sect. 3.2). However, spectroscopic signatures of winds and outflows are detected in all the TTSs. Three types of signatures have been detected in the UV:

The emission profiles of the MgII resonance lines (2796, 2803Å) show a pronounced and broad absorption of their blue-wing in the 16 TTSs observed with IUE or HST (see *e.g.* Gómez de Castro 1997). Blue wing absorption is also observed in Ly α . Terminal velocities up to ~ 300 km s⁻¹ are observed. Unfortunately, the interpretation of these profiles is very complex since the MgII and Ly α lines are optically thick and there is no unambiguous method for determining the underlying blueshifted emission and thus the true wind absorption.

Narrow and blueshifted C III] 1909Å and Si III] 1892Å emission has been detected at the same velocity as the optical jets in some TTSs (Gómez de Castro & Verdugo 2003a). This emission is produced by unresolved jets and indicates that pre-main-sequence jets are hotter than previously

inferred from the optical observations in agreement with the UV observations of protostellar jets and Herbig-Haro objects (see Sect.3.2).

Optically thin semiforbidden lines tracing warm plasma (C II] 2325Å, O II], and, most prominently, C III] and Si III]) show long blueward-shifted tails with velocities up to -300 km s^{-1} as in RU Lup and slight shifts to the blue of the line peak (Gómez de Castro & Verdugo 2003a).

These data provide three key tips: there is a broad range of temperatures in the outflows (3,000 - 30,000 K), outflows are not spherically symmetric and their kinematics produce line broadenings/asymmetries similar to the jet velocity (or terminal velocity of the outflow) in several sources.

The interpretation of the profiles requires a detailed comparison with theory since the kinematics of MHD winds from rotating structures is very complex; three basic motions overlap: rotation, acceleration along the axis and radial expansion from the axis (see Fig 6). Each kinematical component dominates at different locations of the outflow. Rotation is dominant close to the source of the outflow. Further out, radial expansion is the most significant component up to some height, z_0 , above the disk. For $z > z_0$, the dominant kinematical component is acceleration along the disk axis, *e.g.*, a collimated outflow or jet. For standard parameters, the base of the wind is unresolved: $z_0 = 5 \text{ AU}$ (see Gómez de Castro & Ferro-Fontán, 2005). Thus, the only way to track the velocity law of the wind is by a clever selection of spectral indicators based on the thermal properties of the wind.

From a theoretical point of view, three possible types of outflows can be fitted into this broad context: a stellar wind, a disk wind, and an outflow driven from the interface. Either centrifugal stresses or magnetic/thermal pressure are involved in their acceleration, but it is still unclear which is the dominant mechanism whether it is universal, and how this mechanism acts when radiation pressure becomes significant as in Ae/Be Herbig stars. Numerical simulations predict temperatures between $\sim 10,000\text{K}$ for the inner-disk winds up to $\sim 10^{6-7} \text{ K}$ close to the magnetic reconnection boundary (Goodson et al 1997). The X-rays (and the high energy particles) produced in the reconnection areas will be redistributed towards lower energies due to the densities involved. Thus, the dominant radiative output from TTSs winds is expected in the UV range, as observed. UV line profiles calculated using a *simplified* warm disk wind model are shown in Fig 7. Notice that very broad or double peaked profiles centered at the rest wavelength of the line can be produced in the wind (not only in the accretion disk) provided that the inclination is $\sim 90^\circ$. These type of profiles have been observed in some TTSs as AK Sco or RW Aur. As shown in Figure 7, a clever selection of the *UV spectral indicators* helps to study the kinematical structure of the wind. The effect of internal wind extinction by dust lifted from the disk mid-plane can also be traced through the flux ratios of the relevant lines.

Another important aspect of TTSs winds is that a significant fraction of the mass outflow is ejected in a non-stationary manner. The time scales for these ejections range from a few hours (Alencar 2001, Bouvier et al 2003, Gómez

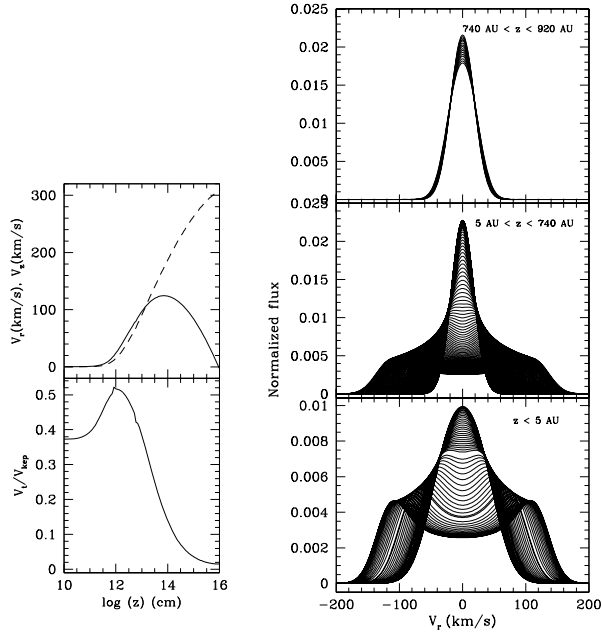


Figure 6: **Left:** Variation of the three velocity components: rotation (V_t), radial expansion from the axis (V_r) and axial velocity (V_z) are represented. *Top panel:* V_z and V_r are represented with dashed and solid lines respectively. *Bottom panel:* The ratio between V_t and the keplerian velocity at 0.1 AU for a solar mass star (155 km/s) is plotted. **Right:** Disk wind kinematics as shown by the line profiles for an edge-on system. Each profile correspond to a ring of gas perpendicular to the outflow axis that is identified by its distance (z) to the disk plane. *Bottom panel:* Line profiles with $z < 5$ AU - the outflow passes from being rotationally dominated (inner broad or double peaked profile) to radial expansion dominated (double peaked profiles with peak velocity ~ 120 km/s. *Middle panel:* outflow passes from being radial expansion dominated to axial-acceleration dominated. *Bottom panel:* outflow is dominated by axial acceleration - line broadening is basically thermal (from Gómez de Castro and Ferro-Fontán, 2005).

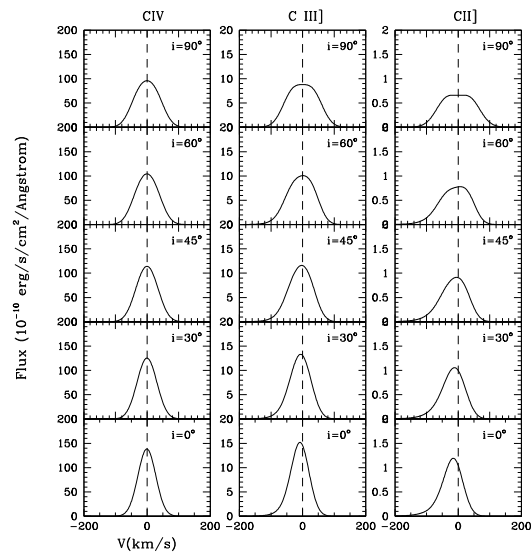


Figure 7: C IV, C III] and C II] line profiles for the unresolved $z < 12$ AU region. The profiles are plotted for inclinations 0° , 30° , 45° , 60° and 90° from bottom to top.

de Castro & Verdugo 2003b) to some ten years (optical jets observations, see *e.g.* López-Martín et al 2003) or even to some hundred of years (molecular gas bullets, see *e.g.* Bachiller 1996). Recent observations have set-up a *lower limit of around 1 hour* precluding the association of flares with the few hours time-scale variability in RW Aur, since the characteristic decay time of flares in active stars is some few hundredths of seconds (Gómez de Castro & Verdugo 2003b). Several ejection time-scales typically co-exist in the same object. For instance, time-scales of ~ 1 h, ~ 5.5 d and ~ 20 yr are observed in RW Aur. Despite the wealth of valuable information that could have been obtained by HST/STIS to determine the kinematics and properties of the outflows, *the observations available in this domain are coarse.*

3.2 UV observations of Herbig-Haro objects and jets

Observations of protostellar jets can provide important clues concerning the collimation mechanism: in particular, the role of episodic ejections or internal shocks in the jet, heat dissipation, and major heating sources. Also, such observations provide important clues on the interaction between the jet and the surrounding molecular gas helping to discriminate between radiation-induced (photodissociation) versus collision-induced (shocks) in the circum-jet chemistry.

Since early in the IUE project, it has been known that protostellar jets and Herbig-Haro objects have a higher degree of ionization than that inferred from optical data (Bohm-Vitense et al 1982, Schwartz et al 1985, see also Gómez de Castro & Robles, 1999 for a compilation). High excitation objects like HH1 or HH2 produce strong emission lines of C IV 1548, 1550Å, OIII] 1664Å, SiIII] 1892Å, and CIII] 1909Å (Ortolonai & D’Odorico 1980). However low excitation objects like HH43 or HH47 are characterized by the presence of the H₂ Lyman band emission lines (Schwartz 1983). H₂ emission lines, which are pumped by the UV radiation generated in the internal shocks of the jet, can be used to measure the strength of the radiation field generated in the shock (and the Ly α line strength).

UV lines are variable and the variation of the low ionization species is anticorrelated with the variations of the high ionization species and the short wavelength continuum. A detailed study of HH 29 combining optical and UV data led Liseau et al (1996) to propose a two phase model with a component at $T = 10^4$ K and $n_e = 10^3$ cm⁻³ and a hot and dense component with $T = 10^5$ K and $n_e = 10^6$ cm⁻³ with a very small filling factor (0.1%–1%).

Using IUE, Bohm et al (1987) and Lee et al (1988) detected a variable and spatially extended short wavelength (1300–1500Å) UV continuum. At the end of the IUE mission, it was believed that the most likely mechanism for its formation was continuum H₂ emission formed in the destruction process of H₂ molecules caused either by photodissociation by radiation shortwards of 912 Å or by collisions with low energy thermal particles. This assumption was based on the absence of the dominant Lyman features (at 1258, 1272, 1431, 1446, 1505, 1547 and 1562 Å) detected in low excitation objects as HH43 or HH47. The

high resolution spectra of HH2 obtained with the Hopkins Ultraviolet Telescope (HUT) has shown that the UV emission below 1620 Å is mostly produced by UV emission from H₂ (H₂ bands are detected below 1200 Å and band structure is observed at 1510 Å, 1580 Å and 1610 Å, see Raymond et al 1997). Unfortunately, this is the *only* high resolution spectrum of a HH object obtained in the far UV (HH47 was observed with HST/GHRS as the spectral coverage is tiny 1262-1298 Å; Curiel et al 1995). A low dispersion ($\simeq 1000$) spectrum of HH47 obtained with HST/FOS/G270H show no significant depletion of Fe in the outflow.

UV observations have left open important questions that cannot be solved without further UV observations. It is still unclear, how the kinetic energy of the flow is damped into radiation. The non detection of O VI emission (Raymond et al 1997) and the simultaneous detection of strong C IV and H₂ emission represent the strongest (henceforth, the most promising) defy to radiative cooling models. Another important issue is to understand the excitation mechanism of the H₂ line radiation: H₂ band structure is observed in high excitation HH objects. Some suggestions have been put forwards as collisional pumping of H₂ levels (Raymond et al. 1997).

3.3 Ae/Be Herbig stars

Ae/Be Herbig stars are pre-main sequence, intermediate-mass (2-10 M_⊙) stars. They are rather puzzling objects. Their larger masses suggest that the gravitational collapse is super-alfvénic so, magnetic fields are not expected to be strong. However, Ae stars have a rich UV emission-line spectrum consistent with the presence of a chromosphere above the photosphere (Brown et al 1996, Deleuil et al 2005). Moreover over-ionized species (transition region or coronal - alike) are observed; marginal detection of magnetic fields has been reported for HD 104237 (Donati et al 1997). Thus observations point out that fields are present, at least, during the first $\sim 5 \times 10^6$ yrs of their pre-main sequence evolution.

UV-optical monitoring campaigns discovered azimuthal structures in the wind of AB Aur (Praderie et al 1986). Further thorough optical monitorings (MUlti-SItE COntinuous Spectroscopic -MUSICOS- campaigns) confirmed the presencen of such azimuthal structures in the wind and in the chromosphere: the rotation period of the chromospheric structures is 32h (the stellar rotation period) while the rotation period of the wind (traced by the UV Mg II lines) is 45h (Bohm et al. 1996, Catalá et al 1999). Further UV observations detected clumps of very hot gas, traced by N V emission, in the wind of AB Aur (Bouret et al 1997). The generation of these azimuthal structures and the very hot clumps is often interpreted by means of a 2-components wind model (somewhat alike the solar wind):

- A “slow” and dense outflow reaching terminal velocities of $\sim 300 \text{ km s}^{-1}$ which produces the prominent P-Cygni profiles observed in the Ca II and Mg II[uv1] lines and the broad, blueshifted absorption observed in

C IV[uv1]. Mass-loss rates derived from semi-empirical models are of some $10^{-8} M_{\odot} \text{ yr}^{-1}$ (Bouret & Catalá, 1998, Catalá & Kunasz, 1987).

A “high” velocity component made by streamers of magnetically confined gas.

As Herbig stars are fast rotators and gas in the streamers is forced to corotate up to the Alfvén point, shocks are expected to occur between the “slow” and the “fast” component. As a result dense azimuthal structures are formed at the corotating interaction regions (CIRs). The existence of a magnetic colimator is further supported by the detection of low density, Ly α jets in HD 163296 and HD 104237 (Devine et al 2000, Grady et al 2004). Magnetic field dissipation also seems the most likely source for the radiative losses in the chromosphere/wind that represent 4%-8% of the stellar bolometric luminosity according to Bouret & Catalá, (1998) although accretion flows may be a non-negligible source (Blondel et al 1983, Bouret & Catalá, 2000, Roberge et al 2001). However, accretion may not be the driver of the outflow. Radiatively driven winds are able to produce collimated outflows provided there is a mild magnetic field (Sakurai, 1985, Rotstein & Giménez de Castro, 1996). The ultimate source of the field remains unidentified: turbulence and rotation could set up a dynamo in the outer layers. Turbulence can be generated by stellar pulsation; radial and non-radial modes have been detected with periods from some tens minutes to hours (see Catalá, 2003 for a review). Also the rotational braking produced by the strong stellar wind could induce turbulent motions below the stellar surface keeping magnetic fields in the outer stellar layers (Lignieres et al 1996).

Further UV observations are required to characterize the winds, the evolution of the hot clumps (so the shocks between the fast and slow components) and to study the physical conditions of the disks. Herbig stars are evolutionary precursors of the Vega-like stars such as β Pictoris (Vidal-Madjar et al 1998) thus they are an ideal laboratory to study planet formation. Radio and IR observations are well suited to map the extended disk structure. Optical and IR coronographic observations with the HST have provided high quality images of the disk structure at large (*e.g.* Clampin et al, 2003). However, UV spectroscopy is the most sensitive tool to determine the column density of hydrogen and the fraction of hydrogen atoms in molecular form (see, for instance, Bouret et al 2003, Grady et al. 2005). H₂ abundance measures the interaction formation rate on dust grains and enhancement of UV photoionizing radiation.

3.4 In summary: the potentials of the UV

It is widely believed that infrared and radio wavelengths are the most appropriate for studying the formation of stars. This perception is based on pre-main sequence stars typically being embedded in molecular clouds that strongly attenuate UV and optical radiation. This statement is true for the early stages of star formation, but after about 1 Myr extinction generally is low and TTSs are accessible to the very powerful ultraviolet diagnostic tools. *To study the evolution of TTS and Herbig stars after 1 Myr is very important*, because planets are formed at this time and the inner disk can be observed while the planets

are forming. Also the basic engine that regulates the formation of stars, the accretion-outflow engine, is naked and can be properly observed.

Examples of some of the diagnostic capabilities of high resolution UV spectroscopy and monitoring are outlined in Figure 8 and Figure 9.

UV line profiles can clearly disentangle accretion from outflow

Figure 8 shows some UV lines in the RY Tau spectrum. The Fe II] 2506Å line shows a broad red-shifted profile with a sharp edge at zero velocity. Since this line is pumped by Ly α photons, it should be formed in the accretion flow. The [O II] 2471Å line is blueshifted and traces the wind (Gómez de Castro & Verdugo, 2005). Both lines are optically thin with no self-absorption effects. For comparison, the strong Mg II 2796, 2802Å lines display absorption components at the wind velocity and an extended red wing associated with the accretion flow. These two physical components could not have been disentangled from the analysis of the Mg II profile alone. In fact, the long red-shifted tail would have been interpreted as a signature of line saturation.

UV monitorings can be used to study the distribution of matter in the circumstellar environment

In the solar system “flares”, *e.g.* sudden increases of the high energy radiation and particles flux, can be produced by at least three very different physical processes: magnetic flares (associated with magnetic reconnection events), corotating interaction regions or CIRs (shock fronts formed in the interaction between the slow and the fast component of the solar wind), and coronal mass ejections. This classification also applies to TTSs and their circumstellar environments. High resolution UV spectroscopic monitorings are required to disentangle the possible mechanisms for flares in proto-stellar systems. This is feasible as shown in Figure 9. AB Dor, a nearby 30 Myr old star, is the only young star that has been monitored. Nine events were detected during the roughly 10 hours monitoring with HST/GHRS! The C IV and Si IV UV line profiles produced by most of the events are narrow and redshifted indicating hot gas falling onto the star during the flare. However, the strongest event produced a very broad profile with narrow absorption slightly blueshifted. This profile lasted some few kiloseconds and thus the broad wings are most likely tracing the front shock of a CIR (Gómez de Castro 2002).

In summary, IUE and HST (with its GHRS or STIS ultraviolet instruments) have allowed us to begin to grasp the enormous potential of the UV spectral range for the study of the physics of accretion and outflow, including the properties of the inner region of protoplanetary disks. Unfortunately, fewer than 10 TTSs were observed with spectral resolution $\sim 50,000$ during the lifetime of these instruments, partly because HST/STIS was not enough sensitive. A UV instrument with sensitivity 50-100 times that of HST/STIS would allow to observe the about 100 TTSs with magnitudes 10-13 located within 160 pc from the Sun (including the fainter and more evolved weak-line TTSs).

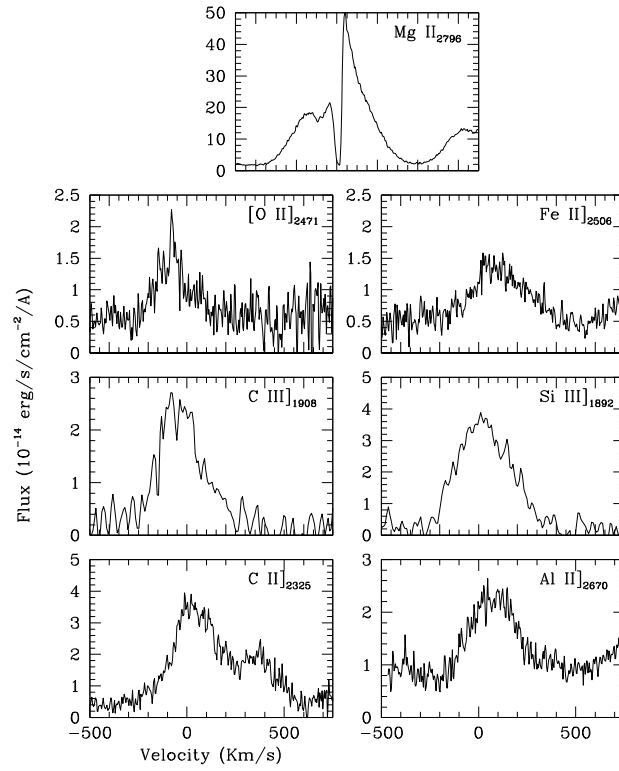


Figure 8: Profiles of some relevant UV lines in the spectrum of RY Tau. The C II] lines are a multiplet with many transitions producing this peculiar profile. All of the lines, except for Mg II, are forbidden or semiforbidden (from Gómez de Castro & Verdugo, 2005).

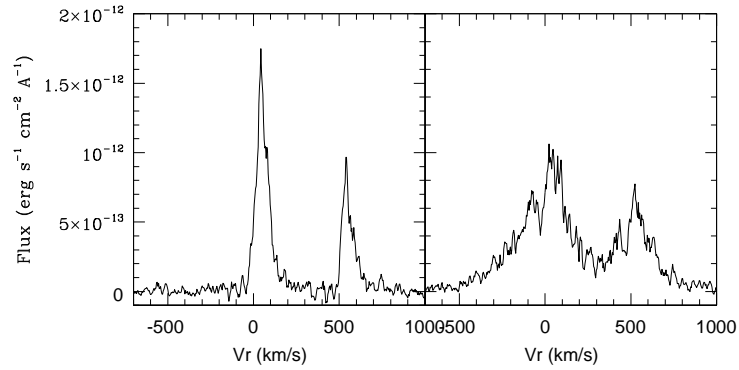


Figure 9: The C IV 1548Å profile of AB Dor during a normal stellar flare (left) and a transient feature probably associated with a CIR (right). Both events lasted few kiloseconds. The left profile is typical of three events that occurred during the short monitoring time, while the profile on the right was observed only once. Note the presence of a narrow absorption and the very broad line wings in the right panel profile (see Gómez de Castro 2002 for more details).

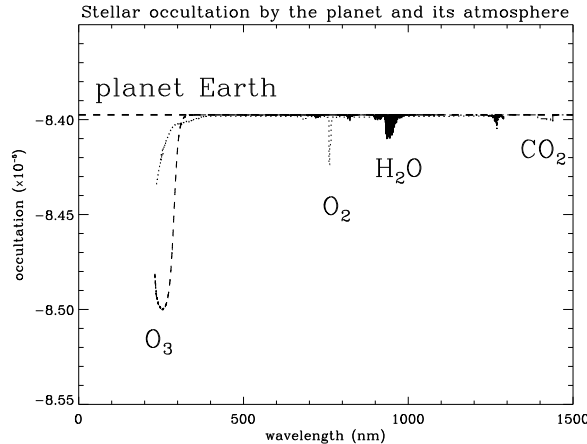


Figure 10: Typical absorption spectrum of an Earth-like planet transiting in front of a Solar-type star from the UV to the near infrared. We assumed the same atmospheric structure as for the Earth with, e.g., similar ozone content. Thin solid, dashed and dotted lines represent H_2O , O_2 and O_3 absorption.

4 Characterization of extrasolar planets atmospheres and search of bio-markers

Since the mid 90's, more than one hundred extrasolar planets have been discovered. In the coming decade, several observing programs will lead to the discovery of an extremely large number of extrasolar planets. To achieve a picture of these new worlds, we need detailed observations of a large sample of these planets. Therefore, we need to be able to characterize planetary atmospheres well beyond the solar neighborhood with reasonable exposure times. The observation of UV and optical absorption when planet transits its parent star is a very powerful diagnostic technique; in fact, the most powerful to detect Earth-like planets, because the strong absorption of stellar UV photons by the Ozone molecule in the planetary atmosphere (see Fig. 10). On-going space missions as Corot, Kepler or GAIA will lead to the discovery of a large number of extrasolar planets transiting its parent star. A new capability for UV spectroscopic observations will be needed for detailed follow-up observations to characterize the extrasolar planets, their atmospheres, and their satellites.

4.1 Extrasolar planets to enlighten the physical processes

Since the unexpected discovery of the first hot-Jupiter (Mayor & Queloz 1995), it is clear that extrasolar planets offer an extremely large diversity. Having more than one hundred extrasolar planets in hand, this diversity is clearly seen in the observed orbital properties of these extrasolar planets. We have “hot-Jupiters”

with orbital periods down to about 3 days, and even, although less numerous, “very hot-Jupiters” with orbital periods down to less than 2 days. Less massive planets have recently been discovered (Santos et al. 2004, McArthur et al. 2004, Butler et al. 2004), and the discussions on their true nature show that a large variety is now expected and certainly possible.

The same variety is also expected concerning the atmospheric content of these planets. A quick look of the atmospheric content and history of the Solar system terrestrial inner planets shows that with 4 planets, we already cover almost the 4 possibilities. Mercury has almost no atmosphere, Mars’ atmosphere is tenuous with about one hundredth of the Earth pressure, and Venus is at the extreme opposite with more than ninety the Earth pressure. Note that Titan, although much smaller than the Earth, has also an atmosphere of 1.5 Bar and is extremely different from other giant planets satellites without atmospheres.

This diversity shows how difficult it is to predict what should be the content of extrasolar planets atmosphere. The Earth is unique with lots of O_2 and O_3 produced by biological activity. Another important characteristics of the Earth atmosphere is the significant presence of water. The Earth and Titan both have lots of N_2 , but Titan has more methane and no O_2 . Mars and Venus have similar atmospheric composition, but their total amounts are in a ratio of more than 10^4 .

As a conclusion, there is no simple answer to the question of the expected characteristics of planets and their atmosphere. In the one hand, the Solar system planets gives a first hint of the expected diversity of the extrasolar planets and their atmosphere. In the other hand, the observations of the extrasolar planets and the detailed characterization of their atmosphere will help to better understand the physical processes at work in the building of a planet and its atmosphere.

It is clear that the detailed processes which made the planets as they are, are still a matter of debate. The impact of many processes are still to be clarified. In short, we do not know the key physical parameters which govern the formation, the evolution and the fate of a given planet and its atmosphere.

What is the impact of the characteristics of the central “Sun” harboring a planetary system (temperature, stellar type, high energy particles flow, metallicity) ? What is the impact of the planetary orbital parameters (orbital distance, eccentricity), the planetary size, mass and potential migration during the formation process ? Are there volatile-rich planets like the proposed “Ocean-planets” ? What is the interaction with the other planets and the planetesimals environment ? This last question is also undoubtedly related to the origin of water on the Earth. Are water-rich planets in the “habitable zone” common, rare, or exceptions ?

Few examples of processes which are believed to play a key role in the building of the planets’ shape can be given. For instance, we can look at the best known planet: our own planet, the Earth. Also still controversial, it is mainly accepted that a primary Earth atmosphere has been accumulated simultaneously with the planet formation. However, the heating of the atmosphere by the young Sun UV and X-ray flux lead to the hydrodynamical escape of this

primary atmosphere (as observed on HD 209458b). Nonetheless, tectonics, volcanism and the planet out-gazing formed a secondary atmosphere in which we live today. Late bombardment by planetesimals in the young planetary system contributed to a large fraction of the Earth water (the exact fraction of water coming from the Earth itself and the outside contribution is still a matter of debate). Finally the life itself enriched the atmosphere in O_2 and ozone, which are therefore considered as atmospheric bio-markers. At least, the observation of O_2 and ozone in the atmosphere of the Earth or any other extrasolar planet can lead to the conclusion that something very particular is happening there. Something which could suggest the presence of life.

It therefore appears that we will soon discover a lot of extrasolar planets. Each one will be different from the others. As soon as we will be able to characterize them in details, a lot of surprises are foreseen. We cannot predict what will be these discoveries. However, this will provide an unprecedented opportunity to better understand the key processes at work in the shaping of planets, and in particular to better understand the origin of our own Earth.

4.2 Ultraviolet observation of transiting planets

In the coming years, many planets will be discovered through transits, for example by the Corot, Kepler, and GAIA missions. In particular, GAIA will likely identify thousands of extrasolar planets transiting bright stars. These will be prime targets for detecting the atmospheric constituents through absorption spectroscopy, thereby characterizing the chemical and physical properties of the atmosphere, including the search for bio-markers, in an extended sample of extrasolar planets.

Many molecules have strong electronic transitions in the UV-optical domain. This wavelength range gives access to the most important constituents of the atmospheres. In particular, bio-markers like Ozone (O_3) have very strong transitions in the ultraviolet (the absorption of UV radiation by the Earth atmosphere is primarily due to O_2 and O_3). The Hartley bands of O_3 are the main absorbers at 200–300 nm. O_2 has strong absorptions in the range 150–200 nm. CO has strong bands below 180 nm, and weaker Cameron bands from 180 to 260 nm. The CO^+ first negative bands are located within the 210 to 280 nm range. Finally, the presence of CO_2 can be detected through the CO_2^+ Fox-Duffenback-Barker bands from 300 to 450 nm. We note also the important presence of O I and C II lines at 1304 and 1335 Å. Observation of these species in the high atmosphere can be easily done, demonstrating that these atoms and ions are present at very high altitude (several hundreds of kilometers) and providing large absorption depths.

The electronic molecular transitions, pumped by UV photons, are several orders of magnitude stronger than the vibrational or rotational transitions observed in the infrared or radio range provided the UV radiation field is strong enough. For this reason, the observation of UV and optical absorption when a planet transits its parent star is an intrinsically more powerful diagnostic technique to characterize the atmospheres of the inner planets than infrared ob-

servations of planetary emission especially, to identify small Earth-like planets. It is far simpler to use the large number of photons in the stellar continuum that are absorbed in spectral lines or molecular bands by the planet’s atmosphere than to try to cancel the huge stellar photon flux by a coronagraph or interferometry to search for the faint infrared emission (thermal and scattered starlight) from the planet. In addition, the intrinsic faintness of the target sources enhances potential difficulties like confusion with exo-zodiacal light. Moreover, observations of the atmosphere of satellites of giant planets, suspected to be numerous, are not feasible in emission.

Presently, the only detections and observations of the atmosphere of an extrasolar planet (HD 209458 b, nicknamed Osiris), have been made through UV-optical spectroscopy, demonstrating that it is an ideal tool to probe the atmospheric content of transiting planets. It is noteworthy that we have in hand 4 detections of an atmosphere of an extrasolar planet (among which the detection of oxygen). All of these present detections have been performed: (1) in space, (2) in the UV-optical wavelength range, and (3) in absorption during planetary transits. This is not a coincidence, but rather a consequence of the method being the most powerful and presenting the best trade-off for the scientific result versus technical feasibility.

4.2.1 Estimates of the expected Earth-like planets detection

For a typical life-supporting terrestrial planet, the ozone layer is optically thick to UV radiation incident at a grazing angle up to an altitude of about 60 kilometers. This ozone layer creates an additional occultation depth of $\Delta F/F \sim 2 \times 10^{-6}$ over hundreds of Angstroms that can be compared to the 2×10^{-4} depth over 1 Angstrom *detected* with HST on HD 209458. We can estimate the minimum brightness of the parent star (F_{\min}) relative to the brightness of HD 209458 (F_{HD209458}) for a detection of the ozone absorption. We have:

$$F_{\min} = \left(\frac{\Delta F/F}{2 \times 10^{-4}} \right)^{-2} \left(\frac{\Delta \lambda}{1 \text{ \AA}} \right)^{-1} \left(\frac{S}{S_{\text{HST/STIS}}} \right)^{-1} F_{\text{HD209458}}.$$

With a telescope 50 times as sensitive as HST/STIS, ozone can thus be detected in earth-like planets orbiting stars brighter than $V \approx 10$ (easily identified by GAIA). This magnitude corresponds to star at a distance $d \sim 50$ pc for the latest type stars considered (K V stars) and more than ~ 500 pc for the earliest stars (F V stars).

With this estimate of the minimum star brightness needed to detect given species, we can evaluate the number of potential targets. The number of targets with planets for which we can probe the atmospheric content, N_{pl} , is simply the total number of stars brighter than the limit N_* , multiplied by the fraction of star having an identified transiting planet at a given orbital range, P_{pl} .

$$N_{pl} = N_* \times P_{pl}.$$

To evaluate the total number of star, the stellar types to be considered is to be defined. The common assumption is to limit the estimates by counting only

K, G and F main sequence stars. This is a conservative assumption based on the bias of the present extrasolar planets discoveries. We used the conservative estimate of

$$N_* = 48\,000 \times 10^{0.6*(V-10)}.$$

The second term of the equation, P_{pl} , is more difficult to quantify with many unknowns. First there must be a planet orbiting the star, second this planet must be identified, and third it must be transiting the stellar disk. We made the assumption that about 25% of stars will have identified orbiting planets in a reasonable future. The probability of a transit for a given planet can be estimated to be $P_{tr} \approx a/R_*$, where a is the orbital distance and R_* is the stellar radius. For a planet orbiting at 1 AU around a solar type star the probability is $P_{tr} \sim 0.5\%$. If we consider the ‘habitable zone’ as the most interesting orbital range, this probability increases for the smaller and more numerous stars. $P_{tr} \sim 0.5\%$ can thus be considered as a conservative assumption for ‘habitable zone’ around solar type stars.

Finally we have an estimate of the number of targets with observable planets:

$$N_{pl} \approx 60 \times 10^{0.6*(V-10)}.$$

A combination of this last equation with the minimum brightness of the parent star needed to detect given species, gives the size of the planet sample that a telescope can analyze as a function of its sensitivity.

Same calculations can be made for exo-planets very different from the Earth. The occultation depth is proportional to the planetary radius (R_p) multiplied by the atmospheric scale height (h). But the scale height is inversely proportional to the planet’s gravity ($g \propto M_p/R_p^2$). These considerations determine that the occultation depth is related to the planet density (ρ_p) by

$$\Delta F/F \propto R_p^3/M_p \propto \rho_p^{-1}.$$

Hence low density planets and planetary satellites will give larger absorption depths than the high density Earth. In short, it is easier to probe the atmosphere through transit spectroscopy in the case of ‘Ocean-planets’ because they are larger, or in the case of ‘Titan-like satellites’, because they are less massive than the Earth and have larger atmospheric scale heights. With an ozone layer similar to that in the Earth’s atmosphere, the occultation depth of an ‘Ocean planet’ or a Titan-like satellite will be $\Delta F/F \sim 5 \times 10^{-6}$. The resulting number estimates of possible detections as a function of the telescope sensitivity are given in Fig. 12.

The estimates of the minimum star brightness to detect the atmospheric signature can be translated into the number of possible detections of atmospheric signatures in transiting planets (n_d). The number of possible detections is related to the number of stars brighter than the minimum brightness ($n(F > F_{\min})$), the probability of finding a planet around these stars (P_p), and the transit probability at a given orbital distance ($P_t(d)$). P_p is unknown and we consider

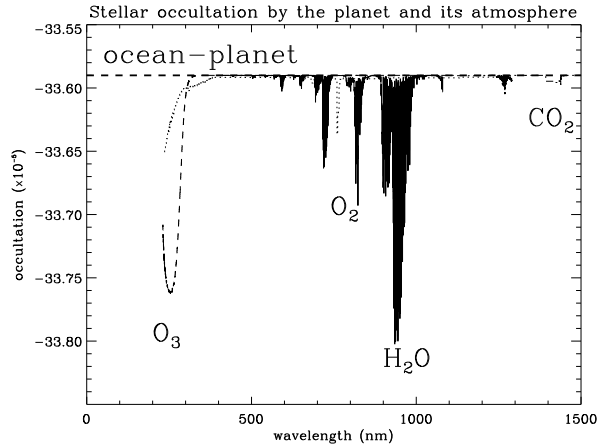


Figure 11: Typical absorption spectrum of an “ocean-planet” as imagined by Leger et al. (2004) when seen transiting in front of a Solar-type star. We assumed the same atmospheric structure as for the Earth but rescaled the structure to the size and density as presently expected for an 6 Earth mass and 2 Earth radius volatile-rich planet.

$P_p = 0.25$ as a reasonable number. We also estimate the transit probability at 1 AU: $P_t(1 \text{ AU}) = 0.5\%$. For the number of stars at a given brightness we restricted to K, G and F type main sequence stars. With these numbers, we plot in Fig. 12 the number of possible detections of atmospheric signatures as a function of the telescope sensitivity. For a UV telescope, the sensitivity depends on the mirror size and the spectrograph efficiency. From now on, we should quote the telescope sensitivity (S) in units of HST/STIS sensitivity because planetary atmospheres have been already detected and studied with this instrumentation and henceforth, we are not limited to a theoretical calculation that may ignore some potential difficulties. We note that a 2 meter class telescope including a spectrograph with the efficiency of the COS instrument leads to a sensitivity $S \sim 20$ HST/STIS.

We see that about *100 extra-solar planets* are expected to transit in front of K, G or F main sequence stars brighter than $V = 10$. In conclusion, using the transit probabilities in the “habitable zone”, we find that the presence of bio-markers and other constituents in the atmospheres can be searched for in more than about 100 Earth-like planets orbiting K, G and F main sequence stars. Further considerations to be taken into account are:

The effect of stellar variety

The number estimates given above can be considered conservative. Indeed, we neglected the stellar type in the estimates and considered the *real* observations of HD 209458b as a benchmark. However, HD 209458 is a G-type star. A very large number of targets will be planets orbiting K-

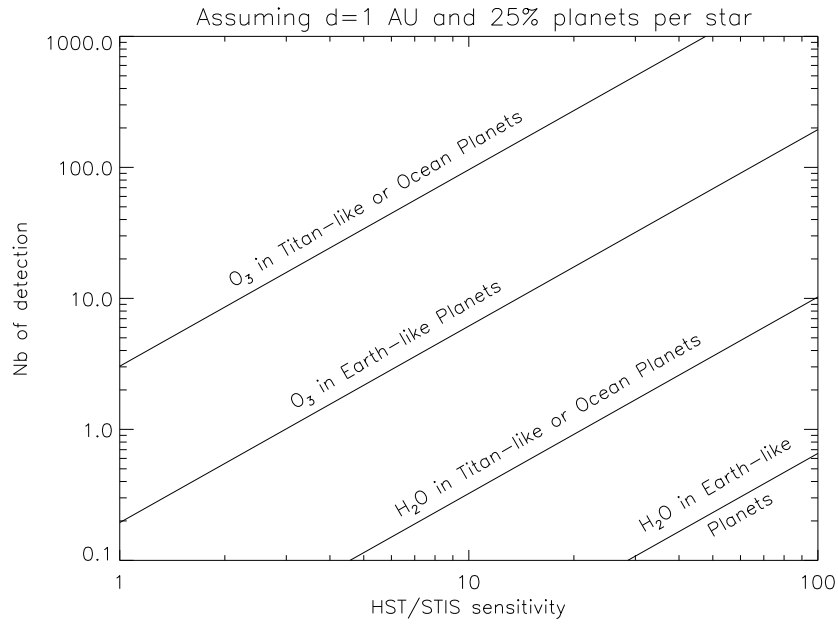


Figure 12: Plot of the number of expected detections of atmospheric signatures as a function of the telescope sensitivity for Earth-like and Ocean-like planets.

type stars. For these stars, the stellar radius is smaller and the absorption depth due the transiting planets will be larger (as observed in the case of the recently discovered planet TrES-1 transiting a K0 V star (Alonso et al. 2004)).

Moreover, late type stars are expected to have habitable zones at smaller orbital distances than the 1 AU assumed in the above calculation. With smaller orbital distances, the transit probability increases and the corresponding number of targets.

Since the previous calculation was done for G-type stars, we expect a larger number of detections for K-type stars. The final number of possible detection of water bands should therefore be larger than mentioned in Fig. 12. Water bands are likely detectable in a reasonable number of Earth-like planets with a 50–100 HST/STIS sensitivity telescope.

The spatial structure of the atmosphere can be studied by time-tagged observations

Absorption spectroscopy of transiting planets can also provide **spatial** information on the physical and chemical properties of their atmospheres. During partial phases when the planet partially covers the observed stellar disk, the time-tagged spectra provide a spatial scan of the planet atmosphere. The partial phase lasts about 10 minutes for an Earth-size extrasolar planet orbiting at 1 AU from its parent star. For the closest stars (≤ 100 parsecs), exposures of a few minutes will allow atmospheric diagnostics of the most important constituents. Detailed time analysis of transit spectra can give information on the spatial distribution of atmospheric characteristics along the planet’s surface, for example, the difference between poles and equator or the spatial inhomogeneity of different chemical constituents.

5 Summary: The needed capabilities

The scientific program outlined in this article requires a broad range of instrumentation from imaging to spectroscopic capabilities.

5.1 Imaging

Two imaging instruments are required: a large field-of-view and a high resolution imager.

The large field of view instrument will be used for two main purposes: mapping of protostellar jets and tracking flares time-scales over large fields.

The high resolution imager primary use is to resolve the cooling structures of jets and to map protostellar disks. Coronagraphy is required. UV provides the best contrast to detected structures around young stars; for instance, a Herbig star is a factor 100 fainter at Ly α than at H α . Narrow filters centered in the

most prominent UV lines like Ly α , C IV, C III, C II, O I, He II or O VI are required.

Any comment about sensitivities?

5.2 Spectroscopy

Most of the science program is oriented towards spectroscopy. Two basic modes are required: high spectral resolution spectroscopy and medium-to-low long-slit spectroscopy.

High resolution spectroscopy ($R \simeq 50,000$) is required for the Doppler based mapping of circumstellar structures, flares, winds and disks. It is also instrumental for detailed studies of the local ISM. The spectral resolving power required to observe the atmosphere of extrasolar planets is not a crucial capability. We have seen that $R = \lambda/\Delta\lambda = 10\,000$ is more than enough. Even lower resolving power, $R < \sim 1\,000$, could be enough to detect the broad band signatures of many molecules.

Note, however, that in some cases, higher resolving power will permit the resolution of thermal broadening of the absorbing lines in the planetary exospheres (Vidal-Madjar et al. 2003). In that case, a high resolving power of $R \sim 100\,000$ will provide important constraints on the atmospheric structure.

Long slit spectroscopy is required to map, the spatially resolved, jet emission, disks and circumstellar envelopes. Spectral resolution as high as 10,000 is required.

Wavelength coverage The target spectral range for the spectroscopic instruments goes from $\sim 1,000\text{\AA}$ (to include the O VI lines and the H₂ bands) to $\sim 4,000$ to get some overlap with optical telescopes and cover most of the molecular broad band absorption expected from extrasolar planets atmosphere. Extension up to $10\,000\text{\AA}$ would give access to the strong “water band” which is of prime interest for the search, statistics and characterization of “habitable planets” and, consequently, for exo-biology.

Sensitivity

An improvement by a factor of 20-100 over HST/STIS capabilities will allow to study the WISM further out the local bubble and get high in the halo towards the High Velocity Clouds. It will also allow to increase the sample of TTSs observed in the UV from some 10 to 200 hundreds, including the weak line TTSs providing, for the first time, an unbiased view of the accretion-outflow engine during pre-main sequence evolution.

In addition, the sensitivity of the spectrograph should be high around prominent nebular lines like CIII], SiIII] or CII].

Time tagged observations

Accurate time information is instrumental. The zero of the time scale needs to be precise to coordinate monitoring campaigns with other instruments or to determine exo-planets transits. The accuracy and uniformity of the time unit sets the spatial resolution for Doppler mapping. Time-tagged observations can be considered as a proxy for spatial resolution at the level of the planet size.

5.3 Orbit

The orbit should be efficient, *e.g.* high, to minimize the effect of Earth occultations, airglow pollution and geocoronal emission and to allow Doppler mapping on time scales of 1 day. An L2 orbit is optimal for this purpose.

This work has been supported by the 6th framework program of the EU through grant ????, by the Ministry of Science and Technology of Spain through grants AYA 2000-966, ESP2001-4637E and ESP2002-10799-E. JLL acknowledges support by NASA through grant AR-09930. MA thanks D. Breitschwerdt for enlightning discussions on non-equilibrium ionization.

Please add your stuff!!!

References

- [] Alencar, S. H. P., Johns-Krull, C. M. and Basri, G., The Spectral Variability of the Classical T Tauri Star DR Tauri, *Astrophysical Journal*, 122, 3335, 2001.
- [1] Ardila, D. R., Basri, G., Walter, F. M., Valenti, J. A. and Johns-Krull, C. M., Observations of T Tauri Stars using Hubble Space Telescope GHRS. I. Far-Ultraviolet Emission Lines, *Astrophysical Journal*, 566, 1100, 2002
- [2] Avillez, M., and Breitschwerdt, D. “Volume filling factors of the ISM phases in star forming galaxies. I. The role of the disk-halo interaction”, *Astronomy & Astrophysics*, in press, 2005
- [3] Avillez, M., and Breitschwerdt, D. “Global Dynamical Evolution of the ISM in Star Forming Galaxies - I. High Resolution 3D HD and MHD Simulations: Effect of the Magnetic Field”, *Astronomy & Astrophysics*, 425, 899, 2004
- [] Bachiller, R., Bipolar Molecular Outflows from Young Stars and Protostars, *Annual Review of Astronomy & Astrophysics*, 34, 111., 1996.
- [4] Benjamin, R., and Shapiro, P., “Nonequilibrium Absorption Line and Emission Spectrum Diagnostics for the Galactic Fountain” in *Ultraviolet and X-Ray Spectroscopy of Laboratory and Astrophysical Plasmas*, ed. E. Silver and S. Kahn, Cambridge Univ. Press, p. 280, 1993

- Bertout, C., Basri, G. and Bouvier, J., Accretion disks around T Tauri stars, *Astrophysical Journal*, 330, 350, 1988
- [5] Breitschwerdt D., and Schmutzler T., “The dynamical signature of the ISM in soft X-rays. I. Diffuse soft X-rays from galaxies”, *Astronomy & Astrophysics*, 347, 650, 1999
- Berghöfer, T.W. and Breitschwerdt, D. The Origin of the Young Stellar Population in the Solar Neighborhood - A Link to the Formation of the Local Bubble?. *Astronomy and Astrophysics*, 390, 299, 2002.
- Blondel, P. F. C., Talavera, A. and Djie, H. R. E. T. A., Lyman alpha emission in spectra of Herbig AE stars - an indication of accretion? *Astronomy and Astrophysics*, 268, 624, 1993.
- Boehm-Vitense, E., Cardelli, J. A., Nemeç, J. M. and Boehm, K. H., The ultraviolet continuous and emission-line spectra of the Herbig-Haro objects HH 2 and HH 1, *Astrophysical Journal*, 262, 224, 1982
- Boehm, T., Catala, C., Donati, J.-F., Welty, A., Baudrand, J. et al, Azimuthal structures in the wind and chromosphere of the Herbig AE star AB Aurigae. Results from the MUSICOS 1992 campaign. *Astronomy and Astrophysics Supplements*, 120, 431, 1996.
- Boehm, K.-H., Buehrke, Th., Raga, A. C., Brugel, E. W., Witt, A. N. and Mundt, R., Ultraviolet spectra of HH 1 and HH 2 - Spatial variations and the continuum problem, *Astrophysical Journal*, 316, 349, 1987.
- Bouret, J.-C., Catala, C. and Simon, T., Nitrogen V in the wind of the pre-main sequence Herbig AE star AB Aurigae, *Astronomy and Astrophysics* , 328, 606, 1997.
- Bouret, J.-C. and Catala, C., Multi-line analysis of the spectra of Herbig Ae/Be stars, *Astronomy and Astrophysics* , 340, 163, 1998.
- Bouret, J.-C. and Catala, C., NLTE calculations of neutral helium lines in the wind of the Herbig Ae star AB Aurigae, *Astronomy and Astrophysics* , 359, 1011, 2000.
- Bouret, J.-C., Martin, C., Deleuil, M., Simon, T. and Catala, C. Far UV spectroscopy of the circumstellar environment of the Herbig Be stars HD 259431 and HD 250550, *Astronomy and Astrophysics* , 410, 175, 2003.
- Bouvier, J., Grankin, K. N., Alencar, S. H. P., Dougados, C., Fernández, M. et al, Eclipses by circumstellar material in the T Tauri star AA Tau. II. Evidence for non-stationary magnetospheric accretion, *Astronomy and Astrophysics*, 409, 169, 2003
- Calvet, N., Basri, G. and Kuhi, L. V., The chromospheric hypothesis for the T Tauri phenomenon, *Astrophysical Journal*, 277, 725, 1984

- Catala, C. and Kunasz, P. B., Line formation in the winds of Herbig Ae/Be stars - The H-alpha line, *Astronomy and Astrophysics*, 174, 158, 1987.
- Catala, C., δ Scuti Pulsations in Pre-main Sequence Stars, *Astrophysics and Space Science*, 284, 53, 2003.
- Cernicharo, J., The Polymerization of Acetylene, Hydrogen Cyanide, and Carbon Chains in the Neutral Layers of Carbon-rich Proto-planetary Nebulae, *Astrophysical Journal*, 608, L41, 2004.
- Clampin, M., Krist, J. E., Ardila, D. R., Golimowski, D. A., Hartig, G. F. et al, Hubble Space Telescope ACS Coronagraphic Imaging of the Circumstellar Disk around HD 141569A *Astronomical Journal*, 126, 385, 2003.
- Curiel, S. Raymond, J. C., Wolfire, M., Hartigan, P., Morse, J. et al, Molecular H 2 Emission in HH 47A: Hubble Space Telescope GHRS and FOC Observations *Astrophysical Journal*, 453, 322, 1995
- [6] Danly, L., Lockman, F. J., Meade, M. R., and Savage, B. D., "Ultraviolet and radio observations of Milky Way halo gas", *Astrophysical Journal Supplement Series*, 81, 125, 1991
- Deleuil, M., Bouret, J.-C., Catala, C., Lecavelier des Etangs, A., Vidal-Madjar, A. et al, New insights in the FUV into the activity of the Herbig Ae star HD 163296 *Astronomy and Astrophysics*, 429, 247, 2005.
- Devine, D., Grady, C. A., Kimble, R. A., Woodgate, B., Bruhweiler, F. C. et al, A Ly α Bright Jet from a Herbig AE Star, *Astrophysical Journal*, 542, L115, 2000.
- Donati, J.-F., Semel, M., Carter, B. D., Rees, D. E. and Collier Cameron, A., Spectropolarimetric observations of active stars, *Monthly Notices of the R.A.S.*, 291, 658, 1997.
- Ferro-Fonán, C., and Gomez de Castro, A.I. On the source of dense outflows from T Tauri stars - I. Photoionization of cool MHD disc winds, *Monthly Notices of the R.A.S.*, 342, 427, 2003
- Glassgold, A. E., Najita, J. and Igea, J., Heating Protoplanetary Disk Atmospheres, *Astrophysical Journal*, 615, 972, 2004.
- Grady, C. A., Woodgate, B., Torres, C. A. O., Henning, Th., Apai, D. et al, The Environment of the Optically Brightest Herbig Ae Star, HD 104237 *Astrophysical Journal*, 608, 809, 2004.
- Grady, C. A., Woodgate, B., Heap, S. R., Bowers, C., Nuth, J. A., et al., Resolving the Inner Cavity of the HD 100546 Disk: A Candidate Young Planetary System? *Astrophysical Journal*, 620, 470, 2005.

- Gomez de Castro, A.I. and Fernandez, M., Ultraviolet spectroscopy of the hotspot in the classical T Tauri star DI Cep: observational indications of magnetically channelled accretion. *Monthly Notices of the R.A.S.*, 283,55, 1996
- Gomez de Castro, A.I. and Franqueira, M., *IUE-ULDA Access Guide No. 8: T Tauri Stars*, ESA Scientific Publication, ESA-SP 1205, 1997a
- Gomez de Castro, A.I. and Franqueira, M., Accretion and UV Variability in BP Tauri, *Astrophysical Journal*, 482, 465, 1997b
- Gomez de Castro, A.I. and Robles, A., *INES Access Guide No. 1: Herbig-Haro Objects*, ESA Scientific Publication, ESA-SP 1237, 1999
- Gomez de Castro, A.I. and Lamzin,S., Accretion shocks in T Tauri stars: diagnosis via semiforbidden ultraviolet line ratios, *Monthly Notices of the R.A.S.*, 304, L41, 1999
- Gomez de Castro, A.I. On the source of the flaring activity in AB Doradus: the UV spectral signatures, *Monthly Notices of the R.A.S.*, 332, 409, 2002
- Gomez de Castro, A.I. and Verdugo, E., Hubble Space Telescope STIS Spectrum of RW Aurigae A: Evidence for an Ionized Beltlike Structure and Mass Ejection in Timescales of a Few Hours *Astrophysical Journal*, 597,443, 2003a
- Gomez de Castro, A.I., Magnetic Activity and the Interaction Between the Stellar Magnetosphere and the Accretion Disk, *Astrophysics and Space Science*, 292,561, 2004
- Gomez de Castro, A.I. and Ferro-Fontán, C. On the source of dense outflows from T Tauri stars. II. Warm disk winds. *Monthly Notices of the R.A.S.*, accepted, 2005
- Goodson, A. P., Winglee, R. M., Boehm, K-H, Time Dependent Outflows from Accreting Magnetic Ysos, *Astrophysical Journal*,489, 199, 1997
- Goodson, A. P., Boehm, K-H, and Winglee, R. M., Jets from Accreting Magnetic Young Stellar Objects. I. Comparison of Observations and High-Resolution Simulation Results, *Astrophysical Journal*,524, 142, 1999
- Guenther, E. W., Lehmann, H., Emerson, J. P.and Staude, J., Measurements of magnetic field strength on T Tauri stars *Astronomy and Astrophysics*,341, 768, 1999
- Gullbring, E., Calvet, N., Muzerolle, J. and Hartmann, L., The Structure and Emission of the Accretion Shock in T Tauri Stars. II. The Ultraviolet-Continuum Emission, *The Astrophysical Journal*, 544, 927, 2000
- Haffner, L. M., Reynolds, R. J., Tufte, S. L., Madsen, G. J., Jaehnig, K. P. and Percival, J. W., “ The Wisconsin H α Mapper Northern Sky Survey”, *The Astrophysical Journal Supplement Series*, 149, 405, 2003

- Hartigan, P., Hartmann, L., Kenyon, S. J., Strom, S. E. and Skrutskie, M. F., Correlations of optical and infrared excesses in T Tauri stars, *Astrophysical Journal*, 354, L25, 1990
- Heyer, M., Zweibel, E., “Turbulence in the Star-forming Interstellar Medium: Steps toward Constraining Theories with Observations”, *Astrophysics & Space Science*, 292, 9, 2004
- Herczeg, G.J., Linsky, J.L., Valenti, J.A., Johns-Krull, C.M., and Wood, B.E. The Far-ultraviolet Spectrum of TW Hydrae. I. Observations of H₂ Fluorescence. *Astrophysical Journal*, 572, 310, 2002.
- Herczeg, G. J., Wood, B. E., Linsky, J. L., Valenti, J. A. and Johns-Krull, C. M., The Far-Ultraviolet Spectra of TW Hydrae. II. Models of H₂ Fluorescence in a Disk, *Astrophysical Journal*, 607, 369, 2004
- Johns-Krull, C. M., Valenti, J. A. and Koresko, C., Measuring the Magnetic Field on the Classical T Tauri Star BP Tauri. *Astrophysical Journal*, 516, 900, 1999
- Kueker, M., Henning, T. and Ruediger, G., Magnetic Star-Disk Coupling in Classical T Tauri Systems, *Astrophysical Journal*, 589, 397, 2003
- Kulkarni, S., Heiles, C. Neutral hydrogen and the diffuse interstellar medium. *Galactic and extragalactic radio astronomy*, Berlin and New York, Springer-Verlag, 1988, p. 95.
- Lallement, R. and Bertin, P. Northern-Hemisphere Observations of Nearby Interstellar Gas - Possible Detection of the Local Cloud. *Astronomy and Astrophysics*, 266, 479, 1992.
- Lallement, R., Welsh, B.Y., Vergely, J.L., Crifo, F., and Sfeir, D., 3D Mapping of the Dense Interstellar Gas Around the Local Bubble. *Astronomy and Astrophysics*, 411, 447, 2003.
- Lauroesch, J.T., Meyer, D.M., and Blades, J.C. Evidence for Interstellar Na I Structure at Scales Down to 15 AU in Low-Density Gas. *Astrophysical Journal*, 543, L43, 2000.
- Lee, M. G., Bohm, K. H., Temple, S. D., Raga, A. C., Mateo, M. L., Brugel, E. W., Mundt, R., The spatial distribution of ultraviolet line and continuum emission in Herbig-Haro objects, *The Astronomical Journal*, 96, 1690, 1988.
- Lignieres, F., Catala, C. and Mangeney, A., Angular momentum transfer in pre-main-sequence stars of intermediate mass, *Astronomy and Astrophysics*, 314, 465, 1996.
- Liseau, R., Hultgren, M., Fridlund, C. V. M. and Cameron, M., Time variable shocks in the UV: long term IUE monitoring of HH 29., *Astronomy and Astrophysics*, 306, 255, 1996.

- López-Martin, L., Cabrit, S. and Dougados, C., Proper motions and velocity asymmetries in the RW Aur jet, *Astronomy and Astrophysics*, 405, L1, 2003.
- Maíz-Apellániz, J. The Origin of the Local Bubble. *Astrophysical Journal*, 560, L83, 2001.
- [7] Martin, C., & Bowyer, S., “Discovery of high-ionization far-ultraviolet line emission from the interstellar medium”, *Astrophysical Journal*, 350, 242, 1990
- Matt, S., Goodson, A. P., Winglee, R. M., Boehm, K-H, Simulation-based Investigation of a Model for the Interaction between Stellar Magnetospheres and Circumstellar Accretion Disks *Astrophysical Journal*, 574, 232, 2002
- [8] McKee, C.F., Ostriker, J.P., “A theory of the interstellar medium - Three components regulated by supernova explosions in an inhomogeneous substrate”, *Astrophysical Journal*, 218, 148, 1977
- [9] Moos, H. W., Sembach, K. R., Vidal-Madjar, A., York, D. G., Friedman, S. D. et al., “Abundances of Deuterium, Nitrogen, and Oxygen in the Local Interstellar Medium: Overview of First Results from the FUSE Mission”, *Astrophysical Journal, Suppl. Series*, 140, 3
- [10] Muzerolle, J., Calvet, N. and Hartmann, L., Emission-Line Diagnostics of T Tauri Magnetospheric Accretion. II. Improved Model Tests and Insights into Accretion Physics, *Astrophysical Journal*, 550, 944, 2001.
- Ortolani, S. and D’Odorico, S., A discussion on the nature of the Herbig-Haro object no. 1 from its far UV spectrum, *Astronomy and Astrophysics*, 83, L8, 1980.
- Petrov, P. P., Gahm, G. F., Gameiro, J. F., Duemmler, R., Ilyin, I. V. et al, Non-axisymmetric accretion on the classical TTS RW Aur A, *Astronomy and Astrophysics*, 369, 993, 2001.
- Praderie, F., Catala, C., Simon, T. and Boesgaard, A. M., Short-term spectral variability in AB Aurigae - Clues for activity in Herbig AE stars. I - The ultraviolet lines of MG II and Fe II, *Astrophysical Journal*, 303, 311, 1986.
- Priest, E. and Forbes, T., *Magnetic reconnection : MHD theory and applications*, New York : Cambridge University Press, 2000.
- Raymond, J.C., Blair, W.P., Long, K.S., Hopkins Ultraviolet Telescope observations of H₂ emission from HH2. *Astrophysical Journal*, 489, 314, 1997.
- Redfield, S. and Linsky, J.L. The Three-dimensional Structure of the Warm Local Interstellar Medium. II. The Colorado Model of the Local Interstellar Cloud. *Astrophysical Journal*, 534, 825, 2000.
- Redfield, S. and Linsky, J.L., The Structure of the Local Interstellar Medium. III. Temperature and Turbulence. *Astrophysical Journal*, 613, 1004, 2004.

- Reynolds, R. J., Chaudhary, V., Madsen, G. J. and Haffner, L. M., “Unresolved H α Enhancements at High Galactic Latitude in the WHAM Sky Survey Maps”, *The Astronomical Journal*, 129, 927, 2005
- Richter, P., Savage, B. D., Wakker, B. P., Sembach, K. R. and Kalberla, P. M. W., “The FUSE Spectrum of PG 0804+761: A Study of Atomic and Molecular Gas in the Lower Galactic Halo and Beyond”, *Astrophysical Journal*, 549, 281, 2001
- Roberge, A., Lecavelier des Etangs, A., Grady, C. A., Vidal-Madjar, A., Bouret, J.-C. et al., FUSE and Hubble Space Telescope/STIS Observations of Hot and Cold Gas in the AB Aurigae System, *Astrophysical Journal*, 551, L97, 2001
- Rotstein, N, Gimenez de Castro, C.G., Radiation-driven Magnetohydrodynamic Wind Solutions for Hot Luminous Stars *Astrophysical Journal*, 464, 859, 1996.
- Sakurai, T., Magnetic stellar winds - A 2-D generalization of the Weber-Davis model *Astronomy & Astrophysics*, 152, 121, 1985
- [11] Savage, B. D., & Sembach, K. R., “Properties of the highly ionized disk and halo gas toward two distant high-latitude stars”, *Astrophysical Journal*, 434, 145, 1994
- [12] Schmutzler, T., and Tscharnuter, W. M., “Effective radiative cooling in optically thin plasmas”, *Astronomy & Astrophysics*, 273, 318, 1993
- Schwartz, R. D., Herbig-Haro objects, *Annual review of astronomy and astrophysics*, 21, 209, 1983
- Schwartz, R. D., Dopita, M.A., Cohen, M., The structure of Herbig-Haro object 43 and Orion dark cloud extinction, *The Astronomical Journal*, 90, 1820, 1985.
- [13] Shapiro P. R., Moore R. T., “Time-dependent radiative cooling of a hot, diffuse cosmic gas, and the emergent X-ray spectrum”, *Astrophysical Journal*, 207, 460, 1976
- Simon, T., Vrba, F. J. and Herbst, W., The ultraviolet and visible light variability of BP Tauri - Possible clues for the origin of T Tauri star activity, *The Astronomical Journal*, 100, 1957, 1990
- Slavin, J.D. and Frisch, P.C. The Ionization of Nearby Interstellar Gas. *Astrophysical Journal*, 565, 364, 2002.
- Tripp, T.M., Wakker, B.P., Jenkins, E.B. Bowers, C.W., et al., “Complex C: A Low-Metallicity, High-Velocity Cloud Plunging into the Milky Way”, *Astronomical Journal*, 125, 3122, 2003

- Valenti, J. A., Johns-Krull, C. M. and Linsky, J. L. An IUE Atlas of Pre-Main-Sequence Stars. I. Co-added Final Archive Spectra from the SWP Camera *The Astrophysical Journal, Supplement Series*, 129, 399, 2000
- Vidal-Madjar, A., Lecavelier des Etangs, A. and Ferlet, R., β Pictoris, a young planetary system? A review. *Planetary and Space Science*, 46, 629, 1998.